

## Selection of image support region and of an improved regularization for non-Cartesian SENSE

Y. Kim<sup>1</sup>, J. Fessler<sup>2</sup>, and D. Noll<sup>1</sup>

<sup>1</sup>Biomedical Engineering, University of Michigan, Ann Arbor, MI, United States, <sup>2</sup>Electrical Engineering, University of Michigan, Ann Arbor, MI, United States

### INTRODUCTION

Compared to the well-behaved, highly localized and equi-spaced aliasing pattern that results from undersampling with Cartesian k-space trajectories, undersampling in non-Cartesian k-space results in a more complex and widespread aliasing pattern, in which all pixels in the reduced sampling image interact with the point spread function of all other pixels in the image. Typically, iterative algorithms are required to reduce the aliasing. Thus, in contrast to Cartesian SENSE, the role of the image support region, referred herein as a ‘mask’ which specifies the reconstruction region of interest, may become a more important factor in non-Cartesian SENSE. Proper selection of a mask can potentially improve the conditioning of the reconstruction by constraining regions that are known to be zero. We investigated how different choice of mask affects the performance of non-Cartesian SENSE reconstruction [1,2] with undersampled, spiral k-space data. To examine the effect of sharp changes around the mask edges as a possible source of image artifact, we also added a regularized term to smooth the edges. We tested the effect of region of support or ‘mask’ on simulation and on time series functional data.

### THEORY

**Size of the Mask:** Non-Cartesian SENSE [1,2] uses an iterative conjugate gradient (CG) algorithm rather than a direct unfolding process. With a reduced acquisition, the image reconstruction process is solving an ill-conditioned problem by minimizing a regularized cost function,  $\Psi(x) = \frac{1}{2}\|y-Ax\|^2 + \beta R(x)$ , where  $y$  is the k-space data,  $A$  is the system matrix including the complex spatial sensitivity maps,  $x$  is the image to reconstruct,  $R(x)$  is the spatial roughness penalty function and  $\beta$  is its regularization parameter. By applying a mask with a properly selected image support region, we can exclude background points from  $x$ , making the system matrix,  $A$ , ‘thinner’ which in turn, can result in a better conditioned reconstruction with fewer unknown variables.

**Smoothness of the Mask:** Although our preliminary experiments indicated that using a tight mask could reduce aliasing artifact, the trade off was an increase in edge artifacts, instead, from the small inaccuracies in the mask size. Thus, we applied the term,  $\|D(b)x\|$ , to the regularization function to increase Tikhonov regularization of the image outside a tight mask, effectively producing a ‘soft’ mask. The resulting cost function is:  $\Psi(x) = \frac{1}{2}\|y-Ax\|^2 + \beta R(x) + \gamma\|D(b)x\|^2$ . Here,  $b$  is a ‘softening function’ that dictates the smoothness around the mask edge and two types of softening functions used in our experiment are shown in Figure 3(top).

### METHODS & RESULTS

To determine the effect of mask size and smoothness on non-Cartesian SENSE, we conducted a simulation using a modified Shepp-Logan phantom image. We also conducted a functional human experiment with a finger tapping task using a 3T GE scanner with an 8-channel head array coil. Alternating two-shot gradient echo spiral-out acquisition, each shot being undersampled by factor of 2, was used as described in TSENSE [3]. Other imaging parameters were TR = 2s, TE = 25ms, 64×64 size, FOV = 22cm and 5-mm thick axial slices. For simulation, the sensitivity map used for generating the simulated k-space data was used during reconstruction, whereas a geometric mean approach [4] was used for human experiment. We used a SENSE implementation similar to [1], which uses the time-segmented NUFFT algorithm and an iterative CG algorithm with the regularization terms described above. The algorithm was stopped after 15 iterations. An error map, which is the difference between images from reduced acquisition and from the one from fully-sampled acquisition, was also shown. To investigate the effect of mask size on image quality, we increased the size of the mask one pixel at a time. Fig 1 shows the resulting image domain errors, where the increased mask size of 0 represents the tightest mask. Blue with circle and red with star line shows the results without and with the softening function, respectively. Fig 2 shows images and corresponding error maps for mask sizes that extend (a)0, (b)1, (c)4 and (d)12 pixels beyond the object where the error maps are rescaled to the same value. The arrow in Fig 2(a) shows a halo effect. Fig 3(top) shows two different softening functions: (a)Step and (b)Butterworth and Fig 3(bottom) shows corresponding error maps within the ROI. The arrows indicate significant differences produced by the two softening functions. Fig 4 shows the effect of softening function (Butterworth) with the error maps on human data (slice containing motor cortices) that are consistent with simulation results. The fMRI results (a)without and (b)with softening function (Butterworth) were number of activated pixels: (a) 33, (b)58, image percent error: (a)6.6, (b)5.1, and time series SNR (tSNR): (a)29, (b)32.

### DISCUSSION & CONCLUSION

Our data suggest that mask size does have impact on the image quality and usually, a moderate mask size extended several pixels beyond the object will produce optimal image quality. Smoother mask edges tend to reduce the aliasing artifact. The tightest mask resulted in a halo effect caused by the overfitting of images around the edge, possibly due to the roughness penalty in reconstruction process itself. In addition to the halo effect, we suspect that the tightest mask would not cover the region of interest sufficiently in the case of patient movement. The error map pattern also changes with respect to mask size: the bigger the mask size, the more aliasing artifact in the center of the object. As demonstrated in Fig 1, the energy of the error map is the lowest at the mask size of 4, i.e., Fig 2(c). Thus, even though smaller masks are better, as suggested in our theory, to reduce the halo or motion effect, while still suppressing the aliasing artifact, it is desirable to increase the mask size by several pixels. As shown in Fig 3 and 4, using a softening function can further reduce aliasing artifacts. Butterworth function is more robust for a variety of mask sizes, possibly due to the rounded edges of the function.

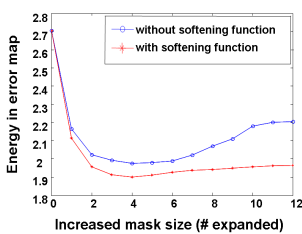


Fig 1. Error map energy within the ROI w.r.t. an increased pixels of mask size. (red) with and (blue) without softening function (Butterworth)

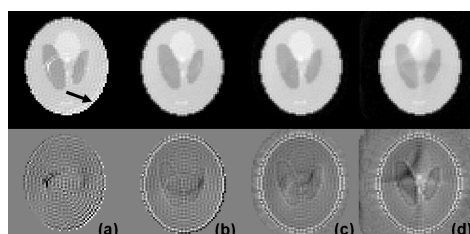


Fig 2. Effect of mask size without smoothing. (top) SENSE images when mask size increased by (a)0, (b)1, (c)4 and (d)12 pixels, respectively, (bottom) corresponding error maps.

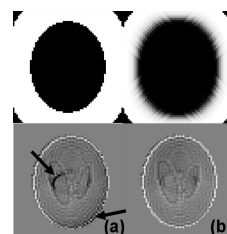


Fig 3. Effect of mask smoothing. (top)Softening functions; (a)Step, (b)Butterworth. (bottom) Error map, mask size of 12

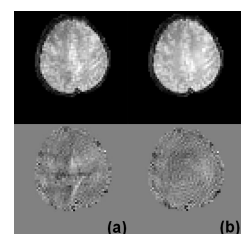


Fig 4. Human experiment. (top) images (a)without and (b)with softening function (Butterworth) (bottom) corresponding error maps and results for fMRI data

**REFERENCES** [1] Sutton, Proc. ISMRM 2001, p771 [2] Pruessmann, MRM 1999;42:952-962, [3] Kellman, MRM 2000;45:846-852, [4] Cao, Proc. ISMRM 2005, p2447  
**ACKNOWLEDGEMENT:** This work was supported by NIH Grants EB002683